JETIR.ORG ISSN: 2349-5162 | ESTD Year : 2014 | Monthly Issue
JOURNAL OF EMERGING TECHNOLOGIES AND INNOVATIVE RESEARCH (JETIR)
An International Scholarly Open Access, Peer-reviewed, Refereed Journal

Study on Tungsten Disulfide Polymorphs Nanomaterials: Properties and Applications

[1]Manu Kumar Bhandoria, [2]Ravi Kumar Rana, [3]Yashpal Sharma, [4]Jitendra Gangwar

[1]Department of Chemistry, [2]Department of Chemistry, [3]Department of Chemistry, [4]Department of Physics
[1,2]Baba Mastnath University, Asthal Bohar, Rohtak, Haryana, India [3,4]RPS Degree College, Balana, Mahendergarh, Haryana, India

Abstract : This study introduces various Nano related terms including Nanoscience, Nanotechnology and Nanomaterials. A brief history and applications of Nanotechnology in different emerging fields are also described in detailed. Classification of Nanomaterials based on their types and dimensionality are elaborated thoroughly. Distinct polymorphs nanomaterials especially metal oxides and transition metal dichalcogenides (TMDs) are selected. A brief description on Tungsten Disulfide (WS_2) nanostructures including 0D, 1D, 2D and 3D nanostructures and polymorphs WS_2 structures is also summarized. A detailed review of literature is proposed in terms of the efficient synthesis, probing capabilities and potential applications of WS_2 nanostructures. Emerging properties in particular electrical, conductivity and mobility, crystallography and optical, as well as potential applications of WS_2 nanostructures are covered in a detailed way. This systematically study provides a new strategy in order to further investigate the unique fundamental properties and to deeply explore their various promising applications.

Keywords **- Nanoscience, Nanotechnology, Nanomaterials, Tungsten Disulfide, Properties, Applications.**

I. INTRODUCTION

1.1 Nanoscience and Naotechnology

In Nanoscience, the prefix 'Nano' derives from the Greek word nanos, which means dwarf or very small, describing the nanoscale (1-100 nanometer) considered suitable for particles and materials. A nanometer (abbreviated as nm) is one-billionth of a meter or one-thousandth of a micrometer or 10^{-9} meter. This is the scale that is often used in measuring atoms and molecules. For example; a hydrogen atom (the smallest elemental particle in nature) has a diameter of about one tenth of a nanometre, six bonded carbon (C) atoms have a width of about one nm, and a human hair has a diameter of about 80×10^3 nm. A typical molecule with the required complexity for nanoscience usually comprises of about 100 atoms and has a diameter in the range of 1 to 10 nm. The development of nanoscience can be traced to the time of the Greeks and Democritus in the 5th century B.C., when scientists considered the question of whether matter is continuous, and thus infinitely divisible into smaller pieces, or composed of small, indivisible and indestructible particles, which scientists now call atoms. The fast growing economy in this area requires experts who have an outstanding knowledge of nanoscience in combination with the skills to apply this knowledge in new products. The word Nanoscience is refers to the study, manipulation and engineering of matter, particles and structures on the nm scale (10^{-9} m *i.e.* the scale of atoms/ions/molecules). Nanoscience is the study of the properties of matter at the nanoscale; in particular, it focuses on the unique, size-dependent properties of solid-state materials [1]. Nanoscience can be carried out by studying particles in glass, as the Romans, Faraday, and Mie did. One can still deduce interesting, size-dependent properties of materials from ensemble, test tube measurements. Nanoscience, therefore, has been around for at least 150 years, ever since the sizes of atoms were first determined. Nanoscience deals with the scientific study of objects with sizes in the 1-100 nm range in at least one dimension. Important properties of materials, such as the electrical, optical, thermal and mechanical properties, are determined by the way molecules and atoms assemble on the nanoscale into larger structures. Moreover, in nm size structures these properties often different then on macroscale, because quantum mechanical effects become more essential.

Nanoscience and Nanotechnology are at the forefront of current modern research. Nanotechnology is the application of nanoscience leading to the use of new nanomaterials (NMs) and nanosize components in useful products. Nanotechnology is the manipulation of matter with at least one dimension sized from 1 to 100 nm, as defined by the National Nanotechnology Initiative (NNI). At this scale (commonly known as nanoscale), the effects especially surface area and quantum mechanical become more prominent in describing properties of matter. The definition of nanotechnology is inclusive of all types of research and technologies that deal with these special properties. Prof. N. Taniguchi, a Japanese scientist (in 1974), was the first to use and define the term "nanotechnology" as "nanotechnology mainly consists of the processing of separation, consolidation, and deformation of materials by one atom or one molecule". The term "nanotechnologies" as well as "nanoscale technologies" is to refer to the broad range of research and applications whose common attribute is size. An earlier description of nanotechnology referred to the particular technological goal of precisely manipulating atoms and/or molecules for fabrication of macroscale products (bulk materials), also

now referred to as molecular nanotechnology. NNI Council of the United States of America (in 2004) describes nanotechnology as "The understanding and control of matter at the scale of nanometre approximately 1 to 100 nm range".

Generally speaking, Nanoscience, a multidisciplinary scientific education, is crucial to provide industry and research institutes with top quality experts who have a generic background in the different sub-disciplines such as Material Science, Physics, Chemistry, Biotechnology, and at the same time be experts in one particular field (as shown in upper segment of Fig. 1), while nanotechnology is the technology of arranging and processing atoms and molecules for the fabrication of materials with nano specifications (as shown in lower segment of Fig. 1).

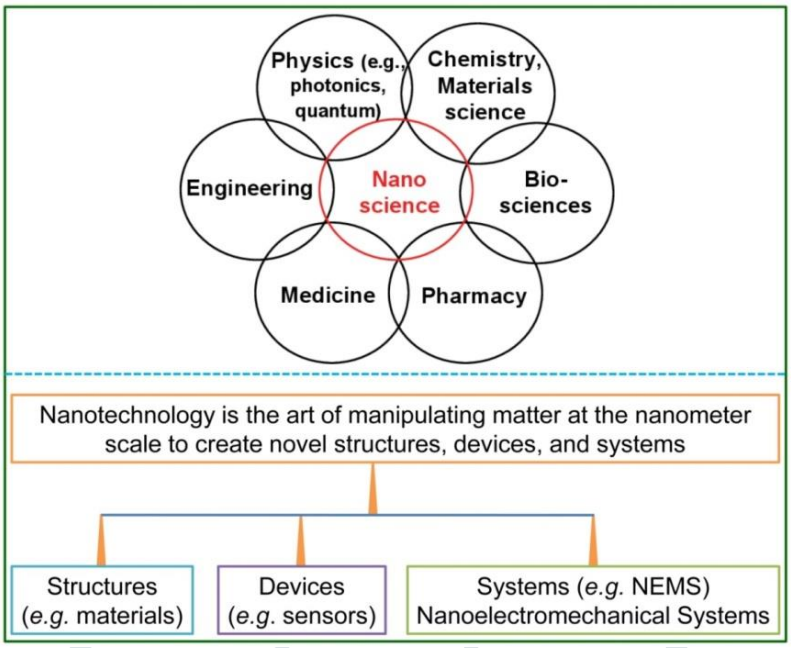

FIGURE 1. A simplified Venn diagram illustrating the cross-disciplinary nature of nanoscience, laying at the intersection of arbitrarily selected disciplines (upper segment) and manipulation of matter at nanoscale for materials, sensors and systems (lower segment).

Nanotechnology is one of the most promising technologies of the 21st century. It is the ability to convert the nanoscience theory to useful applications by observing, measuring, manipulating, assembling, controlling and manufacturing matter at the nm scale. Nanotechnology will eventually provide us with the ability to design custom-made materials and products with new enhanced properties, new nanoelectronics components, new types of 'smart' medicines and sensors, and even interfaces between electronics and biological systems. Nanotechnology may be able to create many new materials and devices with an enormous range of applications, such as in nanomedicine, nanoelectronics, biomaterials energy production, and consumer products. On the other hand, nanotechnology raises many of the same issues as any new technology, including concerns about the toxicity and environmental impact of NMs, and their potential effects on global economics, as well as speculation about various doomsday scenarios.

1.2 Applications of Nanotechnology

Nanotechnology has been employing materials at the nanoscale, which considers a relatively new area for researchers, with rapidly increasing marketable applications which hold the promise of providing important improvements in technologies for protecting the environment and humanity. Nanotechnology is the new field of technological innovation on their application in human biology and medicine. The convergence of nanotechnology and analytical techniques offers great opportunities for the advancement of rapid, miniaturized, ultrasensitive and inexpensive methods for *in-situ* and field-based environmental monitoring. Additionally, the electrocatalytic hydrogen evolution reaction (HER) is now considered a potentially clean method by consuming continuous supplies of electric energy and generates hydrogen, which is regarded as an excellent energy carrier in the future. Moreover, the integration of nanotechnology and biology into nono-sensors and -bionics has greatly increased their potential to sense and identify the environmental conditions. Recently, nanotechnology has been applied in various fields of science with promising results. It offers various diagnostic tools that are less expensive, faster and more sensitive than others. According to recent research, the utilization coefficient of inorganic trace elements was found to be approximately 30%, while nanoparticles are close to 100%. Selenium (Se) nanoparticles have the potential to improve the health of livestock, poultry and fish, as well as promote growth and enhance feed conversion rate, among various aspects [2]. Figure 2(a) shows the size comparison between biological species and different human made nanodevices. Nanotechnology is helping to considerably improve, even revolutionize, many technology and industry sectors including information technology, homeland security, medicine, transportation, energy, food safety, environmental science and among many others. Recently, nanotechnology has been used for a broad range of technical processes, including the characterization, fabrication, and regulation of various materials, in order to develop new materials and to create chemical, biomedical, bioengineering, optical engineering, agricultural, energy, electronic devices, defense and many other innovative applications. Nanotechnology has greatly contributed to major advances in computing and electronics, leading to faster, smaller, and more portable systems that can manage and store larger and larger amounts of information. Figure 2(b) illustrates the innovative applications of Nanotechnology in various fields.

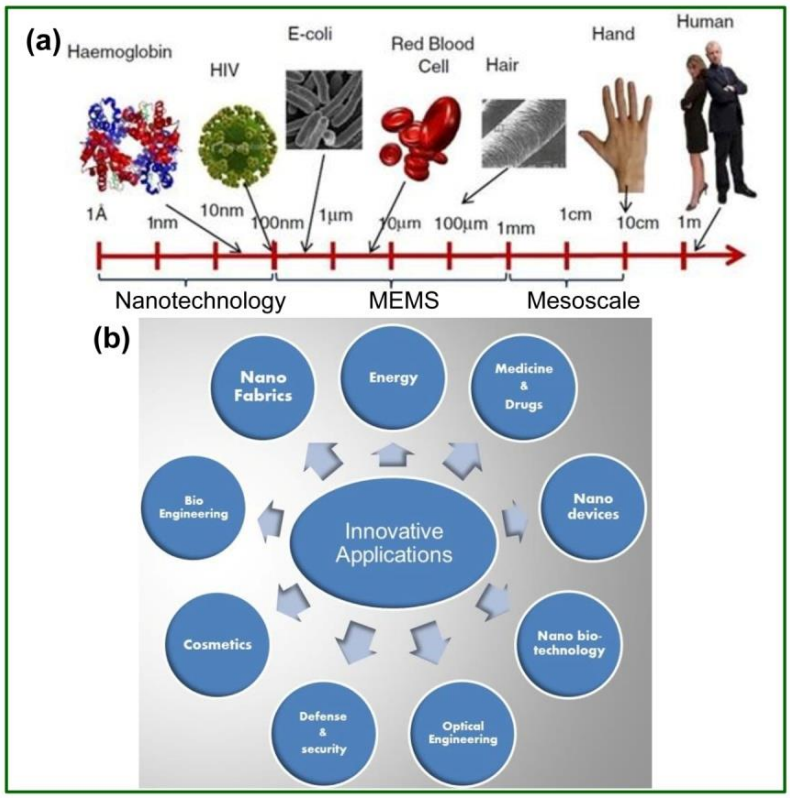

FIGURE 2. Schematically illustration for (a) Size comparison between biological species and different human made nanodevices, and (b) innovative applications of Nanotechnology in various fields. [3]

1.3 Nanomaterials

Nanostructured Materiels or Nanomaterials (NMs) can be defined as the materials possessing, at minimum one external dimension measuring between 1 and 100 nm. The definition given by European Commission (in 2011) which states that the particle size of at least half of the particles in the number size distribution must measure 100 nm or below. NMs are broadly classified into various types based on their origin, size and shape with a diameter of fewer than 100 nm. NMs such as Carbon nanotubes, dendrimers, metal oxides, inorganic materials, polymers, quantum dots and liposomes have been discovered during the last few decades and growing a number of revolutionary novel nanomaterials (as displayed in Fig. 3). The NMs have unique physical, chemical, optical, electronic, mechanical, thermo-physical and many other related properties to their bulk-form counterparts. NMs are slowly becoming commercialized and beginning to emerge as products. NMs have also been developed for use in the military. One example is the use of mobile pigment nanoparticles being used to produce a better form of camouflage, through injection of the particles into the material of soldiers' uniforms. Additionally, the military have developed sensor systems using NMs, such as titanium dioxide (TiO_2), which can detect biological agents. The use of nano-TiO_2 also extends to use in coatings to form self-cleaning surfaces, such as those of plastic garden chairs. A sealed film of water is created on the coating, and any dirt dissolves in the film, after which the next shower will remove the dirt and essentially clean the chairs.

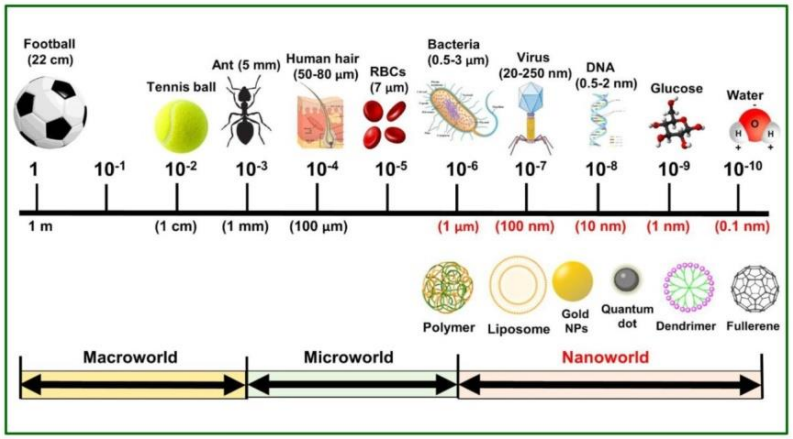

FIGURE 3. Illustration for the length of the relative size of nanomaterials in comparison to naturally occurring things. Some examples of nanoparticles are shown at the bottom of the right corner such as fullerene, dendrimer, quantum dot, Gold nanoparticles, Liposome and polymer nanoparticles.

As there are many different sources of NMs, NMs are classified according to their origin, dimensionality, composition, phases, porosity and dispersion. Based on their origin, NMs can be classified into three main types; (i) engineered, (ii) incidental and (iii) natural NMs.

1.3.1 Nanomaterials Based on Their Dimensionality

NMs are also differentiated from the macroscale materials on their dimensionality (size and morphology) into four main types of NMs; (i) Zero-Dimensional (0D), (ii) One-Dimensional (1D), (iii) Two-Dimensional (2D) and (iv) Three-Dimensional (3D). NMs, therefore, can be classified based on the number of dimensions that are outside the nm scale. The NMs that have all three dimensions in the nanometer scale (smaller than 100 nm) are called 0D NMs, such as inorganic quantum dots, Graphene quantum

dots, carbon quantum dots, fullerenes, magnetic NPs, noble metal NPs and polymer NPs. The NMs that have only one dimension is in nm scale (greater than 100 nm) are known as 1D NMs. For example; metal, metal oxides, and carbon-based 1D NMs with a high aspect ratio especially nanotubes, nanowires, nanorods, nanoneedles, and nanofibers are excellent electron sources that emit electrons in a low electric field. Polymer nanofiber mats, veils, and webs are 1D NMs with large surface-to-volume ratio, elevated porosity and small pores that are exploited for decontamination, catalysis, filtration, and also for super-absorbent NMs for tissue engineering and wound dressings. Carbon nanotubes are a natural semi-1D nanostructure that can be used as a template for synthesis. The materials type that has two dimensions are in nm scale (>100 nm) is classified as 2D NMs. The 2D NMs have sheet-, ribbon- and/or plate-like shapes and have thin layers with a thickness of at least one atomic layer. Additionally, 2D NMs are crystalline materials consisting of a two-dimensional single layer of atoms. Graphene /graphene oxide GO)/ reduced GO (rGO), silicate clays, layered double hydroxides, transition metal dichalcogenides (TMDs), transition metal oxides (TMOs), black phosphorus, graphitic carbon nitride, hexagonal boron nitride (hBN), boron nanosheets, antimonite, and tin telluride nanosheets are some examples of 2D NMs. Thin films with nanoscale thicknesses are considered nanostructures, but are sometimes not considered NMs because they do not exist separately from the substrate. The materials that have all three dimensions in nm scale (>100 nm) are known as 3D NMs.

The class of 3D NMs includes box-shaped grapheme (BSG) nanostructure and bundles of nanowires, and nanotubes. BSG nanostructure is a multilayer system of parallel hollow nanochannels located along the surface and having quadrangular cross-section. The thickness of the channel walls is approximately equal to 1 nm. The typical width of channel facets makes about 25 nm. Some other 3D materials contain features on the nanoscale, including nanocomposites, nanocrystalline materials, nanostructured films, and nanotextured surfaces. Nanoballs, nanocoils, nanopillars, nanocones and nanoflowers are some of the common examples of 3D NMs. Interestingly, both the nanowires and nanorods are 1D NMs, in which there is confinement of electrons in the transverse directions and they are free to move along the length of the wire/rod just as in the bulk material. The aspect ratio (length/diameter) is differs them, nanowires have high aspect ratios up to 1000 while the aspect raio can vary between 2 and 15 in nanorods. The clear difference, thus, between nanowire and a nanorod is due to the different values of aspect ratios for them. Nanowires have much higher aspect ratios as compared to nanorods. The ratio between their diameters to their lengths may be less than 10-3, whereas for nanorods this diameter/length ratio it is in the range 0.1 and 0.3. When the structure are, therefore, made small enough i.e. in the nanometer range, they acquire interesting and useful properties. In nano-regime properties of NMs are quite different as compared to their bulk counterparts.

1.3.2 Polymorphs Nanomaterials

NMs are also categorized into three main types based on their crystallinity; (i) crystalline (long range order and periodicity exists), (ii) non-crystalline (amorphous or glass like; no long range order exists), and (iii) semi-crystalline or polycrystalline (multiple domains, short range order exists). In crystalline NMs, the atoms in crystal are arranged in a periodic manner. However, not all NMs are nanocrystals, indeed some do not display a periodic structure (amorphous solids), and others include many small regions of single-crystal material or polycrystalline solids. In function of their crystal phases, NMs can be classified in single- and multi-phase NMs. In single-phase NM, nanosized materials are contain only one crystal type, whereas various crystals or semicrystalline materials are in multi-phase NMs. Metal NPs are the best example of single-phase NMs, whereas the core-shell NPs and nanocomposites are the examples of multi-phase NMs. Consequently, the properties of individual phases determine the behaviour of such multiphase NMs. The same NMs may exist in both amorphous and crystalline nature, depending on their constituents' arrangement.

The word polymorphism originates from a Greek word. It consists mainly two terms; (i) Polus and (ii) Morph. The term polus is stands for many, whereas the term morph is signify for the shapes, the word Polymorphism, therefore, translates many shapes. Polymorphism is also defined as the ability of a solid material to exist in more than one form crystal structures or phases that have different arrangements or conformations of the molecules in the crystal lattice. In other words, polymorphs materials are the materials with same composition but different crystal structures. The NMs that exhibits polymorphism are classified as polymorphs NMs. Polymorphism is found in any crystalline material including metal oxides, TMDs, polymers, minerals and metals. It is related to allotropy, which refers to chemical elements. A polymorphic transition is a reversible transition of a solid crystalline phase at a certain temperature and pressure (specified as the inversion point) to another phase of the same chemical composition with a different crystal structure. In other words, polymorphs are different in crystal structure but identical in same state or phase. Silica (SiO_2) is known to form many polymorphs, the most important of which are α-quartz, β-quartz, tridymite, cristobalite, moganite, coesite, and stishovite. A classical example is the pair of minerals, calcite and aragonite, both forms of calcium carbonate (CaCo3). Numerous metal oxides and TMDs polymorphs NMs have attracted much attention because these materials are of significant economic value.

As various metal oxides (MOs) exhibit different polymorphs structures, keeping in view crystal structures of few MOs especially TiO_2, Al_2O_3, ZrO_2 and Fe_2O_3 are chosen for this study. For example, TiO_2 polymorphs NMs have rutile-TiO_2, brookite-TiO_2, anatase-TiO_2 and TiO_2(B) phases; Al_2O_3 polymorphs NMs have γ-Al_2O_3, δ-Al_2O_3, θ-Al_2O_3 and α-Al_2O_3 phases; ZrO_2 polymorphs NMs include monoclinic-ZrO_2, tetragonal-ZrO_2, and cubic-ZrO_2 phases; Fe_2O_3 polymorphs NMs elucidate α-Fe_2O_3, β-Fe_2O_3, γ-Fe_2O_3, ε-Fe_2O_3 and ζ-Fe_2O_3 phases [4-10].

Amongst various TMDs polymorphs, MoS_2 and WS_2 NMs are selected for this study. MoS_2 NMs show the hexagonal structure of Mo and S layers present in MoS_2. Three phases of MoS_2 with 1T-MoS_2, 2H-MoS_2 and 3R-MoS_2 have trigonal, hexagonal and rhombohedral crystal structures. Additionally, varied phases of WS_2 with 1T-WS_2, 2H-WS_2 and 3R-WS_2 illustrate trigonal, hexagonal and rhombohedral crystal structures, respectively. Noticeably, it is observed that 1T, 2H and 3R phases have one, two and three number of layers in a repeat unit cell, respectively [11, 12].

II. TUNGESTEN DISULFIDE POLYMORPHS NANOSTRUCTURES

2.1 Tungesten Disulfide Nanostructures

Among various interesting TMSs (such as Ag_2S, CdS, MoS_2, MnS, PbS, TiS_2, WS_2, ZnS and many others), tungsten disulfide (WS_2) is more interesting and distinguishable contender due to inert, good stability, excellent electrical, superior electrocatalytic, electrochemical and environmentally friendly properties as well as abundant active sites, where both the metal (W) and chalcogen

(S) atoms are active electrocatalytically performance [13, 14]. In addition, WS_2 possesses a weak inter-atomic bonding with Van der Waals forces, a large inter-planar spacing ($d_{(002)}$ = 0.616 nm), a lower intrinsic impedance than MoS_2, higher theoretical specific capacity (432 mA h g^{-1}) than the commercial graphite. WS_2 is a semiconducting material with trigonal structure in which the S atoms are situated in the lattice position of a hexagonal close-packed (hcp) structure.

Distinct WS_2 nanostructures materials (nanomaterials), such as WS_2 nanoribbons, WS_2 nanospheres, WS_2 nanoflowers, WS_2 nanoparticles, WS_2 nanorods, WS_2 nanosheets, WS_2 nanofibers, WS_2 nanowires, WS_2 nanotubes, WS_2 nanoplates, WS_2 nanotriangles, WS_2 nanoflakes, and many others have been studied widely and elucidate favourable structural, optical and electrochemical performances [15]. Based on dimensionality, nanostructures of WS_2 are classified into the following four categories; (i) 0D-WS_2 (nanodots), (ii) 1D-WS_2 (nanotubes, nanofibers, nanowires, nanorods, nanoneedles and nanofilaments), (iii) 2D-WS_2 (nanoarrays, nanobelt, nanosheets, nanoplates and nanoribbons) and (iv) 3D-WS_2 nanostructures (nanoflowers, nanospheres, nanoparticles, nanotriangles and nanoflakes).

2.2 Polymorphs WS_2 Structures

The monolayer WS_2 structure has a sandwich structure, where the upper and lower layers consist of chalcogen (S) atoms, and a plane of transition metal ions (W) is sandwiched in between. Depending on the specific stacking of the different layers, many polymorphs, which exhibit rather different properties, are found in WS_2 structure. Typically, there are mainly two types of structure for WS_2, depending on the arrangement of S atoms, (i) stable (2H) phase and (ii) metastable (1T) phase. Here, the digit stands for number of layers per unit cell and alphabet is stands for crystal structure. These two phases of WS_2 possess quite various special and fascinating properties. Such as, 2H-WS_2 has semiconducting nature which is different from 1T-WS_2 with metallic nature. Therefore, 2H to 1T transition impacts most functional properties as the 2H phase is a poor electrocatalyst, but an excellent light absorber with strong photoluminescence, whereas the 1T phase is catalytically very active, and a good electron conductor, however being metallic, it does not show optical absorption or emission properties [16]. Recently, polymorphs WS_2 structure phases are gaining significant attention because of their intriguing metallic and/or semimetallic conductivity, forming high activity toward hydrogen evolution and supercapacitor applications [17]. For 2H-WS_2, the S atoms in the lower layer are lying below those of the upper layers directly, whereas the S atoms of two layers are offset from each other by 30° in 1T-WS_2 [18].

The 1T-WS_2 structures demonstrating a distorted 1T crystal structure of 1T-WS_2 monolayer [19]. The crystal structure of 2M-WS_2 adopts a structure with a W-W zigzag structure along a direction. Here, 2M stands for a monoclinic crystal structure with two layers per unit cell [20]. The hexagonal structure of 2H-WS_2 monolayer has two layers in a single hexagonal unit cell. The electronic properties of 1T-WS_2 and 2H-WS_2 monolayer are very different. The distorted 1T-WS_2 monolayer possess a metallic character, whereas a semiconducting behaviour with a direct bang-gap of about 2 eV is observed in 2H-WS_2 monolayer [19]. In distorted octahedral (1T') crystal phase of WS_2 (1T'-WS_2), a highly asymmetric nature with two adjacent lines of W atoms crowding together to form the unique zigzag chains is exists [21]. Given those thoroughly different properties of different phases of WS_2, the control at the nanoscale of the crystalline phase of the WS_2 is important to achieve the required outstanding properties in the future nano-devices.

III. REVIEW OF LITERATURE

Analyses on the various interesting properties and potential applications in different fields of polymorphs WS_2 nanostructures are investigated by means of numerous researchers and/or scientists working in this field. Due to the outburst of publications in this field, it is not possible to elaborate and discussed all of them. Some of them, therefore, are discussed in detailed on the efficient syntheses, probing capabilities and potential applications of WS_2 nanostructures are as follows:

Mahler, B.; et. al. (2014) have described the development of colloidal synthetic protocols for producing WS_2 nanosheets, presenting not only the usual semiconducting prismatic 2H-WS_2 structure but also the less common distorted octahedral 1T-WS_2 structure, which exhibits metallic behaviour. Modifications of the synthesis method allow for control over the crystal phase, enabling the formation of either 1T-WS_2 or 2H-WS_2 nanostructures. The factors influencing the formation of the two WS_2 nanostructures were studied using XRD, microscopy and spectroscopy analytical tools to characterize them. Finally, the integration of these two WS_2 nanostructured polymorphs investigated into an efficient photocatalytic hydrogen evolution system to compare their behaviour. [19]

Liu, Q.; et. al. (2017) have developed a new bottom-up hydrothermal synthetic strategy to successfully synthesize high stable 1T-WS_2 nanoribbons with an unusual zigzag-chain type superlattice structure. The atomic microscope and synchrotron radiation-based XAFS analysis clearly revealed W-W reconstruction and W-S distorted octahedral coordination in the nanoribbons, which were highly stabilized by ammonia-ion intercalation. The WS_2 nanoribbons exhibited very distinctive features in electrical transport and Raman scattering properties, which significantly differ from semiconducting 2H-WS_2 phase. The described density functional theory (DFT) calculations have been further used to provide better understanding on the correlation between structure and electrical/optical properties. In a nutshell, this presented work will provide a new route to selectively synthesize stable metallic TMD-based nanostructures, thus open a new window to exploring both fundamental researches in layered material science and potential applications for electronics, optics and catalyst. [22]

Dang, H.; et. al. (2019) have synthesized the 1T-WS_2 nanosheets via a facile hydrothermal method and characterized by a series of technologies. The lateral sizes of WS_2 nanosheets were in the range of 100-200 nm. The WS_2 adsorbents showed excellent adsorption performances (210.2 mg g^{-1}) and ultrafast adsorption rate (2 min) toward methylene blue (MB) under ultrasound. The high adsorption capacity was attributed to its multilayer structure and large surface area, which provided more easily accessible adsorption sites for MB. [23]

Heijst, S. E. V.; et. al. (2021) have presented mixed 2H/3R free-standing WS_2 nanostructures displaying a flower-like configuration are fingerprinted by means of state-of-the-art TEM. Their rich variety of shape-morphology configurations is correlated with relevant local electronic properties such as edge, surface, and bulk plasmons. Machine learning is deployed to establish that the 2H/3R polytype displays an indirect band-gap of Eg = 1.6 (+0.3, -0.2) eV. Further, the high resolution electron energy-loss spectroscopy (EELS) reveals energy-gain peaks exhibiting a gain-to-loss ratio greater than unity, a property that can be exploited for cooling strategies of atomically-thin TMD nanostructures and devices built upon them. The findings of this work represent a stepping stone towards an improved understanding of TMD nanomaterials based on mixed crystalline phases. [24]

Song, X.; et. al. (2023) have reported a simple chemical exfoliation method to create a stable, aqueous, surfactant-free, superconducting ink containing phase-pure 1T'-WS_2 monolayers that are isostructural to the air-sensitive topological insulator 1T'-WTe_2. The printed film is metallic at room temperature and superconducting below 7.3 K, shows strong anisotropic unconventional superconducting behaviour with an in-plane and out-of-plane upper critical magnetic field of 30.1 and 5.3 Tesla, and is stable at ambient conditions for at least 30 days. The results show that chemical processing can make nontrivial 2D materials that were formerly only studied in laboratories commercially accessible. [25]

All these pioneered research works were focused on the synthesis and intriguing properties and potential applications of WS_2 nanostructures. In order to develop, hence, the emerging WS_2 NMs, it is enormously important to develop low-cost with high-yield materials with desirable controlled phase formation, morphology and multifunctional properties.

IV. PROPERTIES OF WS_2 NANOSTRUCTURES

Tungsten disulfide is an inorganic chemical compound composed of tungsten (W) and sulfur (S) with chemical formula WS_2. This chemical compound is part of the group of materials called the TMDs. WS_2 occurs naturally as the rare mineral tungstenite. WS_2 material is a component of certain catalysts and actively used for the hydrodesulfurization as well as hydrodenitrification. WS_2 assumes a layered structure similar, or isotypic with MoS_2, instead with W atoms situated in trigonal prismatic coordination sphere (in place of transition metal Mo atoms). Due to this layered structure, WS_2 forms non-carbon nanotubes and nanowires, which were discovered after heating a thin sample of WS_2. Some of the intriguing properties of WS_2 materials are displayed in Table 1.

Table 1: Some intriguing properties of WS_2 materials

Properties	Characteristics	
Chemical Properties	Chemical formula	WS_2
	Empirical Formula	S_2W
	Group	Tungsten 6; Sulphur 16
	Electronic configuration	Tungsten: [Xe] $4f^{14}$ $5d^4$ $6s^2$, Sulphur: [Ne] $3s^2$ $3p^4$
	Appearance	Blue-gray powder
	Solubility in water	Slightly soluble
Electronic Properties	Band gap	~ 1.35 eV (optical, indirect, bulk)
		~ 2.05 eV (optical, direct, monolayer)
Physical Properties	Density	7.5 g/cm^3, solid
	Melting point	1250 °C (2280 °F; 1520 K)
	Molar mass	247.98 g/mol
Magnetic Properties	Magnetic susceptibility (χ)	$+5850\times10^{-6}$ cm^3/mol
Crystallography Properties	Crystal structure	Molybdenite
	Coordination geometry	Trigonal prismatic (W(IV)), Pyramidal (S^{2-})
	Crystal System (Phase)	Trigonal (1T), Hexagonal (2H), Rhombohedral (3R), Monoclinic (2M)
	Space Group (No.)	P63/mmc (194)
	Lattice parameters (2H phase)	a = b = 3.153 Å, c = 12.323 Å α = 90.00°, β = 90.00°, γ = 120.00°
	c/a ratio	3.908
Electrochemical Properties	Specific Capacitance (Cs)	Cs = 70 F/g at a scan rate of 2 mV/s, Cs = 1439.5 F g-1 at current density of 5 mA cm^{-2}
	Energy density	132.7 W h kg^{-1}
	Power density	224.9 W kg^{-1}
Sensing Properties	Biosensors: Linear range for glucose detection	Ranged from 5 to 300 µM (R^2 = 0.99) with detection limit of 2.9 µM.
Optoelectronic Properties	UV photodetector	Response Time: 48 s, Photosensitivity: 80 mAW^{-1}
Uptake capacities for Soft heavy metal ions	For Pb^{2+} metal ions	386 mg g^{-1} for 1048 mg L^{-1} of Pb^{+2} ions in water.
	For Hg^{2+} metal ions	1954 mg g^{-1} for 978 mg L^{-1} of Hg^{+2} ions in water.

WS_2 is one of the TMDs materials that have superior properties as compared with other TMDs. Moreover, WS_2 are considered as new nanostructures that can be used as a new option in bio-nanomedicine. A variety of WS_2 nanostructures elucidate many outstanding physical, chemical, biocompatibility, optical activity, electronic and many other properties that can be exploited in a wide range of various applications.

4.1 Electrical Properties of WS_2 Nanostructures

The electrical characteristics and properties such as conductivity, mobility, and charge carrier concentration of WS_2 nanostructures have been studied intensively for a decade in connection with numerous possible applications in the energy conversion field including energy harvesting and storage. According to a theoretical study, WS_2 has the highest mobility (µ) among the TMSs family, due to its reduced effective mass. A report elucidated that bulk WS_2 exhibits the following electrical parameters; electrical resistivity (ρ) = 3.37 Ω×cm and mobility (µ) = 30 cm^2 V^{-1} s^{-1} and carrier concentration (p) = 7 × 1016 cm^{-3}. It has also been shown that reducing the number of WS_2 layers into a single layer or bilayer leads to improving the electronic mobility. Experimental work on single layer and bilayer WS_2-based FETs demonstrated room temperature electrical mobility 50 cm^2 V^{-1} s^{-1}. The reported carrier concentration of WS_2 nanotubes showed higher value compared to the bulk and thin film with about 3.0×10^{17} to 1.6×10^{18} cm^{-3} [26].

4.2 Conductivity and Mobility of WS_2 Nanostructures

The electrical properties such as conductivity of WS_2 film is of the order of 10^{-3} $(\Omega\times cm)^{-1}$. The plot of log (conductivity) *versus* 1000/T variation for WS_2 thin film grown by the chemical bath deposition technique shows the straight-line nature indicating the

presence of only one type of conduction mechanism in the range of temperatures adopted. The specific conductivity is found to be in the order of 10^{-3} $(\Omega \times cm)^{-1}$. The activation energy is calculated by using Arrehenius relation and obtained from the linear portion of the graphs was found to be of 0.529 eV. Moreover, monolayer WS_2 possesses superior electrical properties with high carrier mobility for both electrons and holes. The interaction of these carriers with lattice vibration, known as phonons, actually dictates the intrinsic transport properties of WS_2. When considering all phonon branches, the room temperature electron and hole mobilities of monolayer WS_2 are found to be 320 and 540 $cm^2\ V^{-1}\ s^{-1}$, respectively. The effective electron and hole masses are determined to be 0.31 m_0 and 0.42 m_0 (m_0 is the mass of a free electron), accordingly. The larger effective mass and mobility of hole designate that the hole transport experiences less scattering with phonons. Additionally, WS_2 has the highest electron and hole mobilities among all MeX_2 (Me = Mo, W; X = S, Se) materials. When only long wave acoustic phonons are considered, monolayer WS_2 would have a room temperature electron mobility of 1103 $cm^2\ V^{-1}\ s^{-1}$. These calculated results suggest that WS_2 has huge potentials as channel materials for high-performance FETs [26]. The Hall mobility for two WS_2 thin films annealed with nickel (Ni) at 850 °C (WS_2 thin film 1) and with cobalt (Co) at 950 °C (WS_2 thin film 2) are obtained [27]. From measurements at different temperatures, both the Hall mobility and carrier concentration are found to be thermally activated. At room temperature, the typical values of conductivity are 5-10 Sm^{-1}. From Hall measurements, both the films annealed with different metals at distinct temperatures are found to be p-type with a carrier concentration of $p \cong 10^{23}\ m^{-3}$ and a Hall mobility (μ_H) = $10\times10^{-4}\ m^2\ V^{-1}\ s^{-1}$.

Interestingly, it has observed that the WS_2 films are photoconductive with an increase of the conductivity under ambient illumination which is of a few percent. The time-dependent photocurrent signal compared to the signal given by a silicon (Si) photodiode, when chopped light hits the material. It presents the presence of long response times, both in the excitation and relaxation processes. At room temperature, when the light is switched off, it lasts a few seconds until the signal reaches the dark equilibrium condition. For few materials, it can take several minutes at low temperature, such behaviour is a characteristic of deep traps. The photocurrent ΔI adopts a sub-linear law as a function of the photon flux (F_0) such that F_0: $\Delta I \sim F_0^{0.5\text{-}0.7}$. The photon flux of the lamp is constant and lies in the energy range between 1.3-2.5 eV. The onset of the photocurrent at 1.35 eV corresponds to the first indirect transitions of WS_2. The two dips in the quantum yield are obtained at the energy of the exciton absorption peaks at 1.94 eV and 2.36 eV are obtained. This lowest quantum efficiency can be related to two recombination paths; (i) the bound electron-hole pairs can recombine before they dissociate in the electrical field and thus do not participate in the conduction processes, and (ii) the electron-hole pairs are generated close to the surface where the recombination rate is enhanced by numerous surface defects, grain edges and/or steps [27].

4.3 Crystallography Properties of WS_2 Nanostructures

As a member of TMDs, WS_2 possesses a sandwich-like structure. Amongst various TMSs, WS_2 possesses a layered crystal structure and each layer containing three atomic planes. Each of atomic planes has hexagonally packed atoms, where the transition metal (W) atom plane is sandwiched between two planes of sulfur (S) atoms, structuring the S-W-S structure. The thickness of each sandwich layer is about 0.6-0.7 nm. No dangling bonds are appeared on the surfaces of each layer, making the surface very stable as well as nonreactive. Moreover, the layers are hold together by weak Van der Waals interaction. The stable coordination of W is trigonal prismatic, which is the case for 2H-phase of WS_2 (2H-WS_2), while for single layer it is 1H-WS_2. The coordination of W can also have the octahedral coordination, which observed in the meta-stable 1T-phase of WS_2 (1T-WS_2). Due to the stacking difference and lattice distortion, other polymorphs are formed. The lattice parameters of 2H-WS_2 categorise to the nonsymmorphic hexagonal with space group $P6_3/mmc$ (D_{6h}^4) that has the space inversion symmetry with lattice parameters a = b = 0.315 nm and c = 1.232 nm. The unit cell of 2H-WS_2 is extended over two layers with S atoms of the second layer sitting on top of the W atoms of the first layer and vice versa. When 2H-WS_2 is thinned down to a single layer, the unit cell contains only one layer, known as 1H-WS_2. Monolayer 1H-WS_2 is composed of one S-W-S stacking unit, which has a threefold rotational axis (*i.e.* c-axis). The W atoms plane becomes the mirror plane for single-layer WS_2. The crystal lattice of monolayer WS_2 belongs to $P\bar{6}m2$ (D_{3h}^1) and the monolayer counterparts lack of the space inversion symmetry. Additionally, it can be inferred that even layer-number WS_2 has the space inversion symmetry while the odd layer-number WS_2 lacks of the space inversion symmetry from the crystal structure [26]. In addition, WS_2 also belongs the *R3m* space group with lattice parameters a = b = 0.315 nm and c = 1.849 nm.

4.4 Optical Properties of WS_2 Nanostructures

As WS_2 has a layered crystal structure, it shows fascinating layer-number-dependent optical properties. It is generally accepted that the optical transitions arise when a photon is absorbed or emitted by the defects. Therefore, optical absorption and/or transmittance were studied to know the existence of intrinsic point defects in WS_2 nanocrystals. Optical properties of WS_2 nanostructures are investigated by the UV-visible (UV-Vis) and Raman spectroscopy techniques. The optical absorption spectra for WS_2 thin films deposited at room temperature were studied by using UV spectrophotometer. The absorption spectrum of as deposited WS_2 film was measured at room temperature in wavelength ranging from 400 nm to 1000 nm [28]. The interpretation of the experimental results is most often performed with the help of simple equation derived for single crystals. The optical energy band-gap, therefore, of WS_2 thin film was evaluated by using the simplest form of equation obeyed at $h\nu > E_g$ given as follows;

$$(\alpha h\nu)^n = A\ (h\nu - E_g)\ = \text{A (h}\nu \text{ - E}_g\text{)} \qquad (1)$$

where α is the absorption coefficient, h is the Planck's constant, $h\nu$ is the energy of the incident photon, A is a constant, n is the nature of optical transitions and E_g is the optical band-gap of the material. The dependence of absorption coefficient on photon energy is very important in studying the energy band structure and the type of transition of electrons [28].

Raman spectroscopy is an effective technique to identify the phases of TMDs. Raman spectroscopy also offers the valuable information regarding the associated vibrations of lattice ions including optical phonons at the centre of the Brillouin zone in the unit cell, while the vibrational, rotational and other low frequency modes of molecules in a system within the irradiated scattering volume. The group theory suggests the following vibrational modes at the centre of Brillouin zone (Γ-point).

$$\Gamma = A_{1g} + 2A_{2u} + B_{1u} + 2B_{2g} + E_{1g} + 2E_{1u} + E_{2u} + 2E_{2g} \qquad (2)$$

where four modes A_{1g}, E_{1g}, E_{2g}^1 and E_{2g}^2 are the Raman active modes. In the monolayer WS_2, E_{2g}^2 mode is absent due to its crystal symmetry (D_{3h} point group). Other than the first order modes at Γ-point, a zone-edge mode which is identified as the longitudinal acoustic modes at M point, LA(M), is also known to be Raman active in the WS_2 system. The $A_{1g}(\Gamma)$ peaks (centred

about 419 cm^{-1}) and $E^1_{2g}(\Gamma)$ peaks (located about 359 cm^{-1}) are observed for WS_2 films grown by pulsed laser deposition (PLD) technique with varying thicknesses of 1, 2 and 3 monolayers (ML). Additionally, it is observed that a red shift is obtained in $A_{1g}(\Gamma)$ peak, while blue shift is for $E^1_{2g}(\Gamma)$ peak, as the thickness of the film decreases. These studies have revealed that the positions and spacing between the characteristic Raman peaks provide the finger print information about the number of layers present in 2D-TMDs. The Raman spectra of WS_2 nanotubes grown by single step sulfurization of W thin films reveal that two different vibrational modes LA(M), E^2_{2g} were observed at around 173 cm^{-1} and 251 cm^{-1}, respectively. For WS_2 thin film grown by PLD technique, the $A_{1g}(\Gamma)$ peak was obtained at about 420 cm^{-1} but for WS_2 nanotubes this mode shifted to 418 cm^{-1}. For WS_2 nanotubes, the S shell possesses a significant amount of radial component out of phase relative to the almost immobile W shell. Consequently, the $A_{1g}(\Gamma)$ mode acts as a breathing like mode for WS_2 nanotubes and the position of this mode was blue-shifted by 2 cm^{-1} in the Raman analysis [29].

V. Applications of WS_2 Nanostructures

In recent years, WS_2 nanomaterials with various structures as WS_2 nanoparticles, nanotubes, nanowires, nanoribbons and nanodots have been used in some medical and biological research. As a result, WS_2 has promising potentials for a wide range of applications in transistors, FETs, sensors, diodes, LEDs, photodetectors, photocatalytic, pulsed lasers, and many other electronic devices. Among various interesting and exciting applications, some of the applications of WS_2 nanostructures are described in detailed as follows.

5.1 Tribological Applications

2H-TMDs provide various tribological applications, either on its own, or as an additive to fluid lubricants. Solid lubricants are used in areas where lubrication fluids cannot be used, for example lubricating high vacuum systems, or in space applications. The WS_2 nanostructures are used as lubricants such as solid lubricants, dry film lubricants and in self-lubricating composite materials. WS_2 nanostructures are mainly effective in environments of high-pressure, -vacuum and -load. Due to its strength and durability, the WS_2 NMs provide outstanding lubrication and coating abilities. The following features of WS_2 that makes it a fascinating choice for various industrial applications.

i) WS_2 is used for industrial applications involving high temperatures and extreme environments. WS_2 is usually designed to function perfectly between -450 °F and +1200 °F.
ii) WS_2 also used as an additive with metal powder or lubricating oil.
iii) For medical industry, WS_2 is used to coat ball bearings for medical devices, nuclear and vacuum laser applications.
iv) Components that have been coated with WS_2 have been found to achieve friction coefficients in ranging from 0.03 to 0.07.
v) The coating can also withstand high pressures. Many industries use WS_2 in applications where pressures are as high 300,000 psi (Pound per square inch).
vi) WS_2 has been used for a number of applications in aerospace, automotive and military. It is used as friction reducing agents for aerospace and aircraft components.
vii) In the injection molding industry, WS_2 helps to reduce the friction during the molding process. The parts do not stick to the mold and release more quickly. WS_2 is also used for chains, end mills, bearings and gear boxes, among many others.

5.2 Fuel Cells

The global reliance on fossil fuels has incited scientists and governing bodies to make the transition from unsustainable to clean energy solutions. A fuel cell consists of two electrodes; (i) a negative electrode (or anode), and (ii) a positive electrode (or cathode), sandwiched around an electrolyte. WS_2 is one of many NMs being researched for its value in the production of fuel cells and other energy storage applications. Various nanostructures of WS_2 are used as the fuel cells of the anode and anode sensors.

The distinct fascinating and unique properties of polymorphs WS_2 NMs, establishing WS_2 to be a top-draw contender for various potential applications. A comparative study of WS_2 nanostructures with distinct morphologies synthesized through different hydrothermal conditions and pH values with their potential applications is summarized in Table 2.

Table 2: A comparative study of WS_2 nanostructures with distinct morphologies synthesized through different hydrothermal conditions and pH values with their potential applications

WS_2 Morphology	Hydrothermal Conditions	pH value (medium)	Applications	Reference
Nanosheets	265 °C for 24 h	-	In UV photodetector.	[14]
Nanorods, Nanosheets, Nanofibers	180 °C for 24 h	6 (HCl or $NH_3.H_2O$)	Industrial and technology application.	[30]
Nanoribbons	220 °C for 48 h	-	For electronics, optics, and catalyst.	[22]
Nanoflowers	180 °C for 4-72 h	6 (HCl or $NH_3.H_2O$)	As an archetypal photocatalytic material.	[31]
Nanoplatelets	150 °C for 12 h	-	Degradation of rhodamine B (RhB) under visible light irradiation.	[32]
Hexagonal platelets	210 °C for 12 h	8 (HCl)		
Nanosheets	230 °C for 24 h	-	Adsorption performance for dye methylene blue (MB) under ultrasound removal from wastewater.	[33]
brain coral-like nanosheets	180 °C for 24 h	2 (oxalic acid)	Application on long-cycle of lithium-sulfur (Li-S) batteries.	[34]

VI. Conclusions

Keeping in view above exciting research, a facile and cost-effective strategy for TMSs polymorphs NMs fabrication is, therefore, of fundamental importance in the advancement of Nanoscience and related technology. In this regard, herein, a unified study on WS_2 polymorphs NMs with emerging properties and potential applications in distinct fields is discussed. Moreover, a

comprehensive investigation for visualizing various crystallographic features in different WS_2 phases is elucidated. These studies not only evidence the structural characteristics influencing the construction of WS_2 polymorphs structures, but also provide an ideal platform for both fundamental and application-oriented research. Additionally, from these analyses, it suggests that this approach is a remarkable importance of polymorphs WS_2, which is very useful in W-S chemistry.

REFERENCES

[1] Mulvaney, P. 2015. Nanoscience vs Nanotechnology–Defining the Field. ACS Nano, 9: 2215-2217.

[2] Kumar, P.; Singh, P.; Chauhan, S.; Swaroop, M. N.; Bhardwaj, A.; Datta, T. K. and Nayan, V. 2023. Nanotechnology for Animal Sciences-New Insights and Pitfalls: A Review. Agricultural Reviews. DOI: 10.18805/ag.R-2620.

[3] Mohammed, W. A. 2019. Review of Therapeutic Applications of Nanotechnology in Medicine Field and its Side Effects. Journal of Chemical Reviews, 1: 243-251.

[4] Zhang, H. and Banfield, J. F. 2014. Structural Characteristics and Mechanical and Thermodynamic Properties of Nanocrystalline TiO2. Chemical Reviews, 114: 9613-9644.

[5] Gangwar, J.; Gupta, B. K.; Kumar, P.; Tripathi, S. K. and Srivastava, A. K. 2014. Time-resolved and Photoluminescence Spectroscopy of θ-Al_2O_3 Nanowires for Promising Fast Optical Sensor Applications. Dalton Transactions, 43: 17034-17043.

[6] Gangwar, J.; Srivastava, A. K.; Tripathi, S. K.; Wan, M. and Yadav, R. R. 2014. Strong Enhancement in Thermal Conductivity of Ethylene Glycol-based Nanofluids by Amorphous and Crystalline Al_2O_3 Nanoparticles. Applied Physics Letters, 105: 063108.

[7] Neetu, Singh, D.; Kumar, N. and Gangwar, J. 2019. Comparative Study of Crystallographic Representation on the Three ZrO_2 Polymorphs: Structural Models, Lattice Planes, Model Electron and Nuclear Densities. Materials Research Express, 6: 1150f8.

[8] Danno, T.; Nakatsuka, D.; Kusano, Y.; Asaoka, H.; Nakanishi, M.; Fujii, T.; Ikeda, Y. and Takada, J. 2013. Crystal Structure of β-Fe_2O_3 and Topotactic Phase Transformation to α-Fe_2O_3. Crystal Growth and Design, 13: 770-774.

[9] Sakurai, S.; Namai, A.; Hashimoto, K. and Ohkoshi, S. 2009. First Observation of Phase Transformation of All Four Fe_2O_3 Phases ($\gamma \rightarrow \varepsilon \rightarrow \beta \rightarrow \alpha$-Phase). Journal of the American Chemical Society, 131: 18299-18303.

[10] Tuček, J.; Machala, L.; Ono, S.; Namai, A.; Yoshikiyo, M.; Imoto, K.; Tokoro, H.; Ohkoshi, S. and Zbořil, R. 2015. Zeta-Fe_2O_3 - A new stable polymorph in iron(III) oxide family. Scientific Reports, 5: 15091.

[11] Ye, M.; Winslow, D.; Zhang, D.; Pandey, R. and Yap, Y. K. 2015. Recent Advancement on the Optical Properties of Two-Dimensional Molybdenum Disulfide (MoS_2) Thin Films. Photonics, 2: 288-307.

[12] Thiehmed, Z.; Shakoor, A. and Altahtamouni, T. 2021. Recent Advances in WS_2 and Its Based Heterostructures for Water-Splitting Applications. Catalysts, 11: 1283.

[13] Nayak, A. K.; Enhtuwshin, E.; Kim, S. J. and Han, H. 2020. Facile Synthesis of N-Doped WS_2 Nanosheets as an Efficient and Stable Electrocatalyst for Hydrogen Evolution Reaction in Acidic Media. Catalysts, 10: 1238.

[14] Shelke, N. T. and Karche, B. R. 2015. Hydrothermal Synthesis of WS_2/RGO Sheet and their Application in UV Photodetector. Journal of Alloys and Compounds, 653: 298-303.

[15] Liu, M. C.; Zhang, H.; Hu, Y. X.; Lu, C.; Li, J.; Xua, Y. G. and Kong, L. B. 2019. Special Layer-Structured WS_2 Nanoflakes as High Performance Sodium Ion Storage Materials. Sustainable Energy Fuels, 3: 1239-1247.

[16] Kosmala, T.; Palczynski, P.; Amati, M.; Gregoratti, L.; Sezen, H.; Mattevi, C.; Agnoli , S. and Granozzi, G. 2021. Strain Induced Phase Transition of WS_2 by Local Dewetting of Au/Mica Film upon Annealing. Surfaces, 4: 1-8.

[17] Kumar, P.; Thakar, K.; Verma, N. C.; Biswas, J.; Maeda, T.; Roy, A.; Kaneko, K.; Nandi, C. K.; Lodha, S. and Balakrishnan, V. 2020. Polymorphic In-Plane Heterostructures of Monolayer WS_2 for Light-Triggered Field-Effect Transistors. ACS Applied Nano Materials, 3: 3750-3759.

[18] Yi, J.; She, X.; Song, Y.; Mao, M.; Xia, K.; Xu, Y.; Mo, Z.; Wu, J.; Xu, H. and Li, H. 2018. Solvothermal Synthesis of Metallic 1T-WS_2: A Supporting Co-Catalyst on Carbon Nitride Nanosheets Toward Photocatalytic Hydrogen Evolution. Chemical Engineering Journal, 335: 282-289.

[19] Mahler, B.; Hoepfner, V.; Liao, K. and Ozin, G. A. 2014. Colloidal Synthesis of 1T-WS_2 and 2H-WS_2 Nanosheets: Applications for Photocatalytic Hydrogen Evolution. Journal of the American Chemical Society, 136: 14121-14127.

[20] Samarawickrama, P.; Dulal, R.; Fu, Z.; Erugu, U.; Wang, W.; Ackerman, J.; Leonard, B.; Tang, J.; Chien, T. Y. and Tian, J. 2021. Two-Dimensional 2M-WS_2 Nanolayers for Superconductivity. ACS Omega, 6: 2966-2972.

[21] Lai, Z.; He, Q.; Tran, T. H.; Repaka, D. V. M.; Zhou, D. D.; Sun, Y.; Xi, S.; Li, Y.; Chaturvedi, A.; Tan, C.; Chen, B.; Nam, G. H.; Li, B.; Ling, C.; Zhai, W.; Shi, Z.; Hu, D.; Sharma, V.; Hu, Z.; Chen, Y.; Zhang, Z.; Yu, Y.; Wang, X. R.; Ramanujan, R. V.; Ma, Y.; Hippalgaonkar, K. and Zhang, H. 2021. Metastable 1T'-Phase Group VIB Transition Metal Dichalcogenide Crystals, Nature Materials, 20: 1113-1120.

[22] Liu, Q.; Li, X.; Xiao, Z.; Zhou, Y.; Chen, H.; Khalil, A.; Xiang, T.; Xu, J.; Chu, W.; Wu, X.; Yang, J.; Wang, C.; Xiong, Y.; Jin, C.; Ajayan, P. M. and Song, L. 2015. Stable Metallic 1T-WS_2 Nanoribbons Intercalated with Ammonia Ions: The Correlation between Structure and Electrical/Optical Properties. Advanced Materials, 27: 4837-4844.

[23] Dang, H.; Chen, L.; Chen, L.; Yuan, M.; Yan, Z. and Li, M. 2019. Hydrothermal Synthesis of 1T-WS_2 Nanosheets with Excellent Adsorption Performance for Dye Removal from Wastewater. Materials Letters, 254: 42-45.

[24] Heijst, S. E. V.; Mukai, M.; Okunishi, E.; Hashiguchi, H.; Roest, L. I.; Maduro, L.; Rojo, J. and Boj, S. C. 2021. Illuminating the Electronic Properties of WS_2 Polytypism with Electron Microscopy, Annals of Physics, 533: 2000499.

[25] Song, X.; Singha, R.; Cheng, G.; Yeh, Y. W.; Kamm, F.; Khoury, J. F.; Hoff, B. L.; Stiles, J. W.; Pielnhofer, F.; Batson, P. E.; Yao, N. and Schoop, L. M. 2023. Synthesis of an Aqueous, Air-Stable, Superconducting 1T'-WS_2 Monolayer Ink. Science Advances, 9: eadd6167.

[26] Lan, C.; Li, C.; Ho, J. C. and Liu, Y. 2021. 2D WS_2: From Vapor Phase Synthesis to Device Applications. Advanced Electronic Materials, 7, 2000688.

[27] Ballif, C.; Regula, M. and Lévy, F. Optical and Electrical Properties of Semiconducting WS_2 thin films: From Macroscopic to Local Probe Measurements. Solar Energy Materials & Solar Cells, 1999, 57, 189-207.

[28] Hankare, P. P.; Manikshete, A. H.; Sathe, D. J.; Chate, P. A.; Patil, A. A. and Garadkar, K. M. 2009. WS_2 Thin Films: Opto-Electronic Characterization. Journal of Alloys and Compounds, 479: 657-660.

[29] Hossain, E.; Rahman, A. A.; Bapat, R. D.; Parmar, J. B.; Shah, A. P.; Arora, A.; Bratschitsch, R. and Bhattacharya, A. 2018. Facile Synthesis of WS_2 Nanotubes by Sulfurization of Tungsten Thin Films: Formation Mechanism, and Structural and Optical Properties. Nanoscale, 10: 16683-16691.

[30] Cao, S.; Liu, T.; Hussain, S.; Zeng, W.; Peng, X. and Pan, F. 2014. Hydrothermal Synthesis of Variety Low Dimensional WS_2 Nanostructures. Materials Letters, 129: 205-208.

[31] Cao, S.; Liu, T.; Zeng, W.; Hussain, S.; Peng, X. and Pan F. 2014. Synthesis and Characterization of Flower-like WS_2 Nanospheres via a Facile Hydrothermal Route. Journal of Materials Science: Materials in Electronics, 25: 4300-4305.

[32] Vattikuti, S. V. P.; Byon, C. and Chitturi, V. 2016. Selective Hydrothermally Synthesis of Hexagonal WS_2 Platelets and their Photocatalytic Performance under Visible Light Irradiation. Superlattices and Microstructures, 94: 39-50.

[33] Nguyen, T. P.; Nguyen, D. L. T.; Nguyen, V. H.; Le, T. H.; Ly, Q. V.; Vo, D. V. N.; Nguyen, Q. V.; Le, H. S.; Jang, H. W.; Kim, S. Y. and Le, Q. V. 2020. Facile Synthesis of WS_2 Hollow Spheres and their Hydrogen Evolution Reaction Performance. Applied Surface Science, 505: 144574.

[34] Xiong, M.; Qian, J.; Yang, K.; Chen, Z.; Mei, T.; Wang, J.; Li, J.; Yu, L. and Wang, X. 2020. Efficient Polysulfide Anchor: Brain Coral-like WS_2 Nanosheets. Journal of Materials Science, 55: 12031-12040.